Available online at www.sciencedirect.com
SCIENCE DIRECT®
Journal of Molecular Catalysis A: Chemical 208 (2004) 273–284
JOURNAL OF MOLECULAR CATALYSIS A: CHEMICAL
www.elsevier.com/locate/molcata

Selective dehydrolinalool hydrogenation with poly(ethylene oxide)-*block*-poly-2-vinylpyridine micelles filled with Pd nanoparticles

Natalia V. Semagina[a,1], Alexei V. Bykov[a], Esther M. Sulman[a], Valentina G. Matveeva[a], Stanislav N. Sidorov[b], Lidia V. Dubrovina[b], Peter M. Valetsky[b], Olga I. Kiselyova[c], Alexei R. Khokhlov[c], Barry Stein[d], Lyudmila M. Bronstein[e,*]

[a] *A. Nikitin street 22, Tver Technical University, Tver 170026, Russia*
[b] *Nesmeyanov Institute of Organoelement Compounds, Moscow 117813, Russia*
[c] *Physics Department, Moscow State University, Moscow, Russia*
[d] *Department of Biology, Indiana University, Bloomington, IN 47405, USA*
[e] *Department of Chemistry, Indiana University, 800 E. Kirkwood Av., Bloomington, IN 47405, USA*

Received 21 May 2003; received in revised form 24 July 2003; accepted 31 July 2003

Abstract

Selective dehydrolinalool (3,7-dimethyloct-6-ene-1-yne-3-ol, DHL) hydrogenation to linalool (3,7-dimethylocta-1,6-diene-3-ol, LN, a fragrant substance) was studied with Pd nanoparticles formed in poly(ethylene oxide)-*block*-poly-2-vinylpyridine (PEO-*b*-P2VP) micelles with varying solvent composition ('isopropanol (*i*-PrOH):water' ratio) and the pH of the reaction medium. According to transmission electron microscopy (TEM) and atomic force microscopy (AFM), isopropanol fraction and KOH loading control the micellar characteristics governing catalytic properties. The larger and denser the micelles, the slower the reaction due to internal diffusion limitations within the micelles. Denser micelle cores provide better modification of the Pd nanoparticle surface with pyridine units and higher selectivity. The highest selectivity (99.4%) was obtained at pH of 9.4 and 95 vol.% of isopropanol. The highest observed TOF value was found to be 24.4 s^{-1} at pH of 13.0 and 70 vol.% of isopropanol. KOH and isopropanol were shown both to affect the micelle characteristics and act as modifiers of the catalyst surface. The hydrogenation kinetics was studied and zero order with respect to dehydrolinalool was found.

Keywords: Nanoparticle; Poly(ethylene oxide)-*block*-poly-2-vinylpyridine; Hydrogenation; Linalool

1. Introduction

In recent years, catalysis with metal nanoparticles has drawn considerable attention due to enhanced catalytic activity and selectivity of nanostructured catalysts [1–3]. The unique features of metal nanoparticles are significantly influenced by such parameters as metal nanoparticle size, organization of the nanoparticle crystal lattice, nanoparticle surface, (amount of defects) [4] and the chemical nature of the microenvironment surrounding the nanoparticle [5]. Normally catalytic nanoparticles are formed on the inorganic support surface or carbon which do not allow a precise control over nanoparticle size and morphology [6,7]. In this respect, use of nanostructured polymeric matrices as a medium for metal nanoparticle formation results in the improved stabilization of the particles and the enhanced control over particle characteristics [8–13]. Among nanostructured polymers, block copolymer micelles have a number of advantages as they provide soluble systems, yet allow controlling the nanoparticle size, shape, and morphology [14–16].

Hydrogenation of different unsaturated molecules is often used to estimate catalytic properties of nanostructured catalysts [17–19]. A reaction of interest is selective (partial) hydrogenation of triple carbon–carbon bond to double one which is normally catalyzed on palladium [20] and used in synthesis of linalool (3,7-dimethylocta-1,6-diene-3-ol, LN) [21]. Linalool is a fragrant substance of the terpenic

* Corresponding author. Tel.: +1-812-855-3727; fax: +1-812-855-8300.
E-mail addresses: semagina@bio.tstu.tver.ru (N.V. Semagina), lybronst@indiana.edu (L.M. Bronstein).
[1] Co-corresponding author. Tel.: +7-0822-449317; fax: +7-0822-449317.

1381-1169/$ – see front matter © 2003 Elsevier B.V. All rights reserved.
doi:10.1016/S1381-1169(03)00541-7

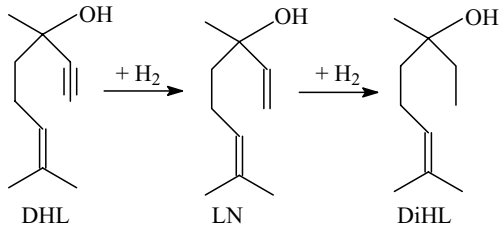

Fig. 1. Scheme of DHL hydrogenation.

series used in several scent compositions and cosmetic preparations. According to [22], linalool is produced in an amount of 6000 tonnes per year. It is also an intermediate in the syntheses of Vitamins A and E, geraniol, citral [23] and exhibits antimicrobial activity [24]. Linalool can be produced via selective hydrogenation of dehydrolinalool (3,7-dimethyloct-6-ene-1-yne-3-ol, DHL) (Fig. 1). If hydrogenation goes on non-selectively, dihydrolinalool (3,7-dimethyloct-6-en-3-ol, DiHL) forms as well. A commercial Lindlar catalyst (palladium deposited on $CaCO_3$ and modified with lead diacetate) is normally used along with quinoline (adsorbed on the catalyst) [25], providing the selectivity of 95% at 100% DHL conversion. Pd catalyst modification achieved via pyridine and quinoline addition to the reaction mixture led to the selectivity of 98.9% at 100% conversion in DHL hydrogenation [26]. Both insufficient selectivity (for Lindlar catalyst) and use of the modifiers polluting the end products and having an unfavorable impact on the environment do not satisfy the modern production requirements.

Recently, we reported catalytic behavior in linalool synthesis of palladium [27] and bimetallic (PdAu, PdPt, and PdZn) nanoparticles formed in the polystyrene-*block*-poly-4-vinylpyridine (PS-*b*-P4VP) micelles in toluene [28]. High selectivity (up to 99.8% linalool) was attributed to modification of the nanoparticle surface with pyridine units of the P4VP micelle core which provided permanent modification of the nanoparticles due to formation of organometallic active center. Electron-donating compounds such as organic bases (piperidine, pyridine) are known to increase selectivity in alkyne hydrogenation [29,30]. Increasing electron density on Pd leads to decreasing interaction with electron-rich compounds. In so doing, the decreased alkene adsorption would favor its desorption and increased selectivity [22]. The drawback of the above block copolymer is use of toluene for micelle formation, implying significant environmental limitations. In this paper, we report exploration of a different block copolymer, poly(ethylene oxide)-*block*-poly-2-vinylpyridine (PEO-*b*-P2VP), for Pd nanoparticle formation, as PEO-*b*-P2VP forms micelles in water and its mixtures with alcohols. The obvious advantage of water–alcohol (especially, ethanol, and isopropanol (*i*-PrOH)) mixtures before toluene is an environmental factor [31,32]. Besides, water addition to the solvent (e.g. ethanol or isopropanol, traditionally used in hydrogenation over Lindlar catalyst [33]) will lead to economic benefit in linalool production due to lower cost of water–alcohol mixtures than that of pure organic solvent. Similar to PS-*b*-P4VP, in PEO-*b*-P2VP, Pd nanoparticles grow surrounded by pyridine species, as the core-forming block is P2VP. At the same time, there is an important difference between these two block copolymer systems. As the P2VP block is pH sensitive [34], in polar medium (water or its mixtures) pH may strongly influence the micellar characteristics which should correlate with catalytic properties giving an important tool in tailoring the catalytic activity and selectivity. The amphiphilic nature of DHL complies with the chosen system.

The present paper reports catalytic properties in selective hydrogenation of DHL to LN using Pd nanoparticles formed in PEO-*b*-P2VP micelles. Correlations between catalyst structure and catalytic properties at different pH and solvent compositions are described. As a second solvent (additive to water), isopropanol was chosen, because it is a good solvent for DHL [33] and, in combination with water, allows keeping micelles intact. As previously reported [35], alkali media (KOH addition) favors the acetylene alcohol hydrogenation, so the reaction was studied in the pH range of 9.4–14.3.

2. Experimentals and methods

2.1. Materials

PEO_{350}-*b*-$P2VP_{135}$ (M_n^{PEO} = 15,400, M_n^{P2VP} = 14,100, M_w/M_n = 1.04) was purchased from Polymer Source Inc., Canada, and used as received. Na_2PdCl_4 was received from Aldrich and used without purification. Dehydrolinalool (99% purity) was supplied by pharmaceutical company OAO "Belgorodvitaminy" (Belgorod, Russia) and distilled under vacuum (40–45 °C at 50–60 kPa). Propan-2-ol (isopropanol) was obtained from Aldrich and distilled before use. KOH and hydrogen (KhimMedService, Tver, Russia) were used as received. Saturated alkali solution was prepared at 25 °C. Water was deionized in a milli-Q purification system.

2.2. Catalyst synthesis

Synthesis of metallated micellar catalyst was carried similar to a method described elsewhere [36]. For this, 0.1156 g of PEO-*b*-P2VP (5.25×10^{-4} mol P2VP) was dissolved in 30 ml water and stirred for 24 h. The block copolymer solution was charged with 1.75×10^{-4} mol (0.0515 g) of Na_2PdCl_4 and stirred for 48 h (molar ratio N:Pd = 3:1). To ensure the absence of the salt outside of the micelle cores, reaction solution was ultrafiltrated using Amicon device. Reduction of Pd ions was carried out by addition of a two-fold excess of an aqueous $NaBH_4$ solution (1 g/l) prepared directly before use. After that, solution was subjected to ultrafiltration to remove all impurities.

2.3. Methods

Measurements of pH were performed with laboratory pH-meter (Ionometer I-160, OO "Izmeritel", Gomel, Byelorussia).

Specimens for transmission electron microscopy were prepared by placing a drop of reaction solution (no dilution) onto a carbon-coated copper grid. Images were acquired at accelerating voltage of 60 kV on JEOL JEM1010.

Atomic force microscopy experiments were performed in tapping mode using the Nanoscope^{TM} IIIa (digital instruments, USA) multimode scanning probe microscope. Commercially available standard silicon 125 μm tapping mode cantilevers (Nanoprobe ^{TM}) were used. The resonant frequency was in the interval 300–350 kHz, the scan rate was maintained 1.5–2.0 Hz. The samples were applied onto freshly cleaved mica surface and left to dry in air at room temperature. Image processing and presentation was done with the help of user-friendly software Femtoscan^{TM}001 (Advanced Technologies Center, Russia).

For the estimation of micelle radii using AFM data, the lateral dimensions of the corresponding protrusion measured at half of its height were taken. These data give the overestimated value, which is due to the finite probe tip size. The explanation of this broadening effect, conventional in probe microscopy, can be found in [37]. The vertical dimensions of the protrusions were not taken as the estimated size, since it was evident that the micelles were slightly distorted (≅20%) presumably due to the deformation on the substrate. The exception was sample 1, containing micellar aggregates, which were strongly deformed on the surface; their vertical dimensions being more than an order of magnitude less than lateral ones. In that case, the radii of particles in the solution were evaluated considering the surface area of micellar aggregates to remain unchanged and using simple geometrical formulae. The surface area of micellar aggregates in AFM images was calculated using the Femtoscan^{TM}001 software options.

Micelle sizes in solutions were examined by spectra turbidity method using photoelectrical colorimeter FEK-56M (Russia) equipped with the high-pressure mercury–quartz lamp (DPK-120) [38,39]. Using a number of filters, the turbidity τ and optical density D were obtained. In the limited range of wavelengths λ at 315–600 nm, spectral dependence of the turbidity can be expressed using Angstrom equation

$$\tau = A\lambda^{-n}, \quad (1)$$

where n is the wave exponent that is the function of relative particle size, α, and relative particle refractive index, m. To find n, experimental data on τ and D were plotted in double logarithmic coordinates and n was found as a slope. Using correlations of n and M_n in a wide range of α and m, particle radius was calculated using

$$r_w = \frac{\alpha \times \lambda_{av}}{2\pi\mu_l}, \quad (2)$$

where μ_l is the refractive index of the dispersion medium and λ_{av} the average wavelength found from equation:

$$\lambda_{av} = \sqrt{\lambda_{max} \times \lambda_{min}} \quad (3)$$

2.4. Hydrogenation of DHL

The catalytic reactions were carried out in a glass batch isothermal reactor installed in a shaker and connected to a gasometric burette. The reactor was equipped with two inlets: for catalyst, solvent, and substrate loading and for hydrogen feeding. *i*-PrOH–water mixture (with different ratios) was used as a solvent (total volume was 30 ml). Saturated solution of KOH was added to the catalyst–solvent mixture to achieve necessary pH values. Prior to the substrate loading, this mixture was saturated with hydrogen in situ for 60 min at the reaction temperature. The substrate-to-catalyst ratio (SCR, mol DHL/mol Pd) was varied by changing the initial substrate concentration (C_0) and catalyst amount (C_c). The experiments were carried out at atmospheric pressure at different temperatures (T). At least three runs were performed under each set of reaction conditions to ensure reproducibility, then data on activity and selectivity were averaged in each time point and standard deviations were calculated.

If not indicated otherwise, effective stirring (960 oscillations/min) was allowed to eliminate the external diffusion effect. Usually sufficiently small heterogeneous catalyst grain [40] allows excluding the internal diffusion as well, but a polymeric matrix in polymer-based hydrogenation catalysts may be responsible for transport limitations [41], hence, a priori we cannot assert that in all the experiments conducted, the effective stirring provides a kinetic regime. Nevertheless, the kinetic studies are free of transport limitations as will be proved below.

The samples were withdrawn from the reactor and analyzed by using a gas chromatograph "CHROM-5" equipped with FID and a glass column 3 m/3mm. The column was filled with solid phase "Chromaton N" (0.16–0.20 mm) saturated with carbowax 20 M (10% of liquid phase to support weight).

3. Results and discussion

3.1. Catalyst synthesis and characterization

Unlike micellar solutions of PS-*b*-P4VP in organic solvents (toluene), where normally metal salt is insoluble (it is solubilized solely in the micelle core due to interaction with pyridine units), PEO-*b*-P2VP block copolymer presents more complex case, as many metal salts (including Na_2PdCl_4 used in this research) are water-soluble. Then the probability of the existence of metal salts outside of the micelle cores is higher. As stated in Section 2, the reaction solution before reduction was ultrafiltrated to remove the Na_2PdCl_4 excess which was not consumed by micelles.

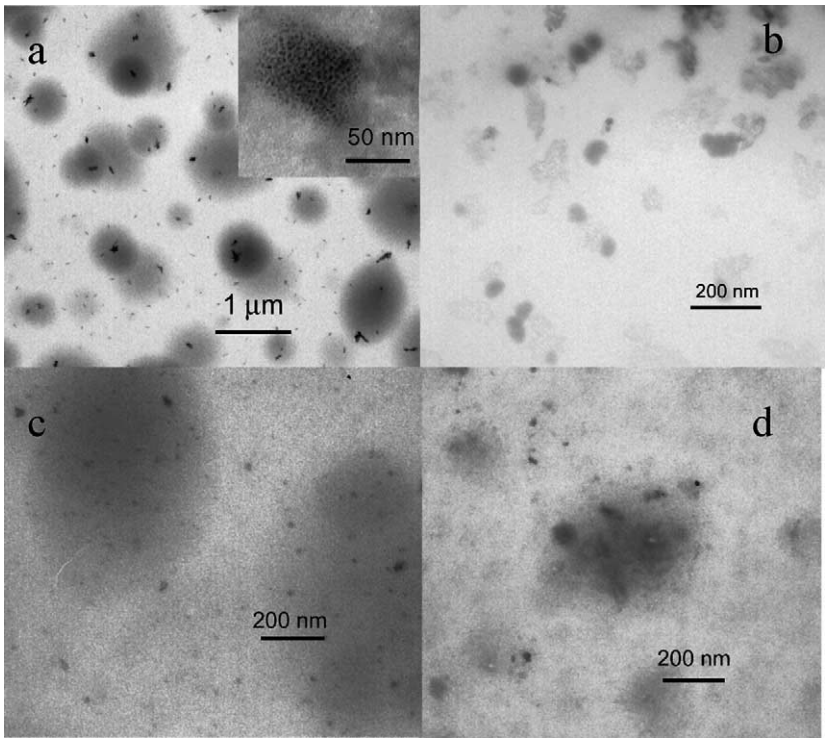

Fig. 2. TEM images of the samples 13 (a), 2 (b), 3 (c), and 4 (d) (see Table 1 for notations). Inset in (a) shows high magnification image.

However, aqueous solution coming out of the ultrafiltration device was found to be colorless. By elemental analysis data, Pd content in the final polymer was 13.13 wt.% (the calculated Pd content corresponding to the Na_2PdCl_4 loading is 13.82 wt.%). So, apparently the micelle cores consume the major part of the Pd salt. Another proof of the Pd species location was obtained from TEM data. Inset in Fig. 2a shows PEO-*b*-P2VP micelle filled with Pd nanoparticles. The latter have a mean diameter of 2.5 nm. As discussed in [36], the mean 'PEO-*b*-P2VP + Na_2PdCl_4' micelle diameter is 81 nm that does not differ from the diameter of the micelles without metal salt. The micellar characteristics of the 'PEO-*b*-P2VP + Pd nanoparticle' samples in different *i*-PrOH–water mixtures are discussed below.

3.2. Catalytic behavior in DHL hydrogenation

3.2.1. Effects of solvent composition and pH

As solvent can influence the reaction rate or selectivity via variation of the solubility of reaction mixture components and interaction with catalytic species [42], the effect of both solvent composition (different '*i*-PrOH:water' volume ratios) and pH of the reaction mixture on the catalytic activity and selectivity was studied. Table 1 contains data on the activity and selectivity in DHL hydrogenation at different pH and *i*-PrOH content in the solvent. Activity was calculated as an average value for 100% DHL conversion that allowed comparing with other reported data on the activity in hydrogenation [5,43].

Runs 1–4 (Table 1) present the data obtained at a fixed pH value (13.4). Selectivity values increase with the increasing *i*-PrOH content. For runs 1 and 2, the catalyst displays practically the same selectivity but the activity increases with increase of *i*-PrOH content, while subsequent alcohol addition leads both to the selectivity and activity increase (runs 2 and 3). Moreover, for runs 3 and 4, a little change in the *i*-PrOH content (5%) results in considerable activity deterioration and selectivity increase. Such effects can not be explained by the catalyst surface modification with a reaction mixture component (*i*-PrOH) as typically done to understand the additive influence [44].

To clarify the pH influence, we carried out the hydrogenation experiments at the optimal *i*-PrOH content (70 vol.%) varying the KOH solution loading (i.e. pH value). One can see (runs 3 and 5–8, Table 1) that the activity and selectivity pass through a minimum (runs 6 and 7, respectively). Inorganic base (KOH) [35], and alkali metal ions [45] are known as promoters of selective acetylene hydrogenation via inducing electron transfer to Pd. At the same time, here increase in KOH amount does not necessarily lead to the selectivity increase, e.g. in runs 3 and 6 the higher the pH value, the lower both the activity and selectivity. Thus, the pH influence cannot be simply explained by geometric or electronic modification of the catalyst surface with KOH [46].

Table 1 contains also data on some other experiments carried out at different pH and *i*-PrOH contents. Runs 9–12 show that pH increase from 10.2 to 12.1 and from 9.9 to 13.4 for 90 and 100% *i*-PrOH, respectively, leads to the activity deterioration, although one should notice that for

Table 1
Catalytic activity and selectivity of Pd nanoparticles formed in PEO-*b*-P2VP micelles depending on the solvent composition and pH[a] and micellar characteristics of the key reaction mixtures obtained from AFM

Run	pH	*i*-PrOH content (vol.%)	Selectivity to Ln[b] (%)	Activity (mol DHL/(mol Pd s))	Mean micelle diameter[c] (nm)
1	13.4	40	95.7 ± 0.4	8.58 ± 0.04	–
2	13.4	50	95.9 ± 0.3	9.21 ± 0.02	34
3	13.4	70	97.8 ± 0.2	9.56 ± 0.02	70
4	13.4	75	98.7 ± 0.2	6.82 ± 0.01	28
5	13.0	70	97.7 ± 0.3	11.00 ± 0.03	–
6	13.9	70	96.8 ± 0.4	7.32 ± 0.03	86
7	14.1	70	98.3 ± 0.5	6.93 ± 0.03	–
8	14.3	70	98.0 ± 0.2	9.22 ± 0.02	–
9	10.2	90	98.5 ± 0.4	4.18 ± 0.02	–
10	12.1	90	–[d]	–[d] (1.57 ± 0.01[e])	–
11	9.9	100	98.7 ± 0.3	2.78 ± 0.01	–
12	13.4	100	–[d]	–[d] (2.33 ± 0.01[f])	144
13	9.4	95	99.4 ± 0.3	5.68 ± 0.02	256
14	9.4	98	98.8 ± 0.2	5.40 ± 0.01	–
15	14.1	80	98.1 ± 0.3	7.81 ± 0.02	–

[a] Reaction conditions: 960 oscillations/min, 70 °C, C_c: 1.72×10^{-5} mol Pd/l, C_0: 0.4 mol/l, and solvent: '*i*-PrOH + water' (30 ml). The key mixtures contain the same quantities of catalyst, DHL, solvent, and KOH for pH adjustment.
[b] At 100% DHL conversion.
[c] Mean diameters for the samples 2, 4, 6, 12, and 13 were calculated out of 200 micelles from AFM images; for the sample 3, 182 micelles were used for calculation and micellar aggregates were not taken into consideration.
[d] 100% conversion was not achieved.
[e] At 61.8% DHL conversion.
[f] At 3.2% DHL conversion.

these compositions, the rates are the lowest among the all studied. *i*-PrOH content increase leads to some activity and selectivity decrease for runs 13 and 14, while for runs 7 and 15 this change results in the activity increase at the same selectivity that indicates once again a combined and complex influence of a pH and water–alcohol ratio on the catalytic properties.

Since micellar characteristics of the PEO-*b*-P2VP–Pd block copolymer aggregates in a given solvent and at a given pH may influence the catalytic properties, this is another important variable for the present system. As discussed above, PEO-*b*-P2VP forms micelles in water which characteristics are mainly preserved after metallation (incorporation of a metal salt and metal nanoparticle formation) [36]. Since there is a possibility of internal mass transfer limitation due to diffusion through the micelle [5], experimental data of Table 1 may include specific rates which were not obtained in the kinetic regime. At the same time, one can assume that at certain micelle characteristics (size and density) mass transfer limitations may be eliminated. This is analogous to the typical test in heterogeneous catalysis on the influence of catalyst grain size on the reaction rate [47]. In order to find micellar characteristics providing a kinetic regime, TEM and AFM studies of the six key reaction mixtures were performed. Table 1 contains mean diameters of the micelles and micellar aggregates obtained from AFM for the samples 2–4, 6, 12, and 13. Figs. 2 and 3 show TEM images of these samples. Figs. 4–9 show AFM images and

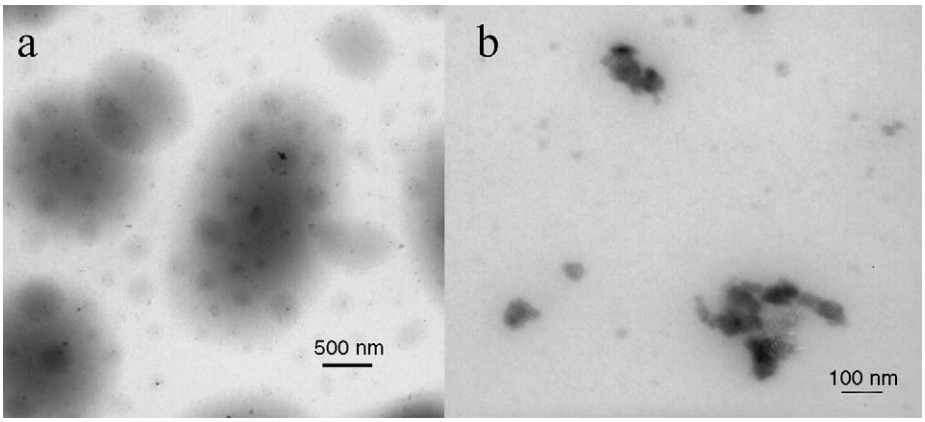

Fig. 3. TEM images of the samples 6 (a), and 12 (b) (see Table 1 for notations).

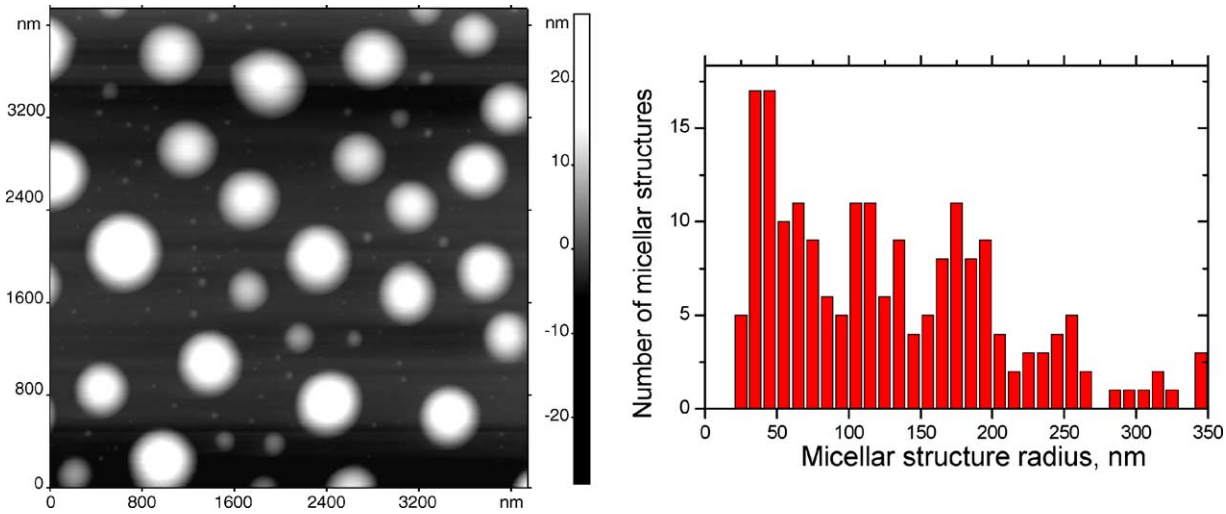

Fig. 4. AFM image (left) and size histogram (right) for the sample 13 from Table 1. The radii of particles in the solution were evaluated considering the surface area of micellar aggregates to remain unchanged and using simple geometrical formulae (see Section 2).

corresponding size histograms (showing radii) of the same micellar structures. One should notice that Table 1 lists mean diameter values instead of radii (obtained from AFM measurements) for easier comparison with TEM data.

As proposed above, size and density of micellar structures should influence the catalytic activity and selectivity. The higher the density and the larger the size of micellar structures, the slower the rate of the substrate and *i*-PrOH penetration to the active sites (internal diffusion limitations), hence, the slower the reaction should proceed. (density of the micelles and micellar aggregates can be derived from the electron density (darkness in the TEM image) of these structures). At the same time, when micelle cores are denser, the local concentration of the pyridine ligands on the particle surface is higher, so the particle modification is stronger. As discussed in our preceding papers [27,28], modification of the metal nanoparticle surface with pyridine units causes the selectivity gain due to electron donation to Pd resulting in decreased strength of LN adsorption [22], thus, increase of the micelle density may increase the selectivity of DHL hydrogenation.

From Fig. 2a one can see that sample 13 contains huge micellar aggregates measuring up to 800 nm and very dense, irregular shape micelles (see inset) with dimensions of 70–80 nm. This combination produces one of the lowest activity and highest selectivity (Table 1). AFM image (Fig. 4) confirms formation of large micellar aggregates with mean diameter of 256 nm. Sample 2 (Fig. 2b) shows no large aggregates, while nearly spherical micelles measuring from 15 to 45 nm form small asymmetric clusters

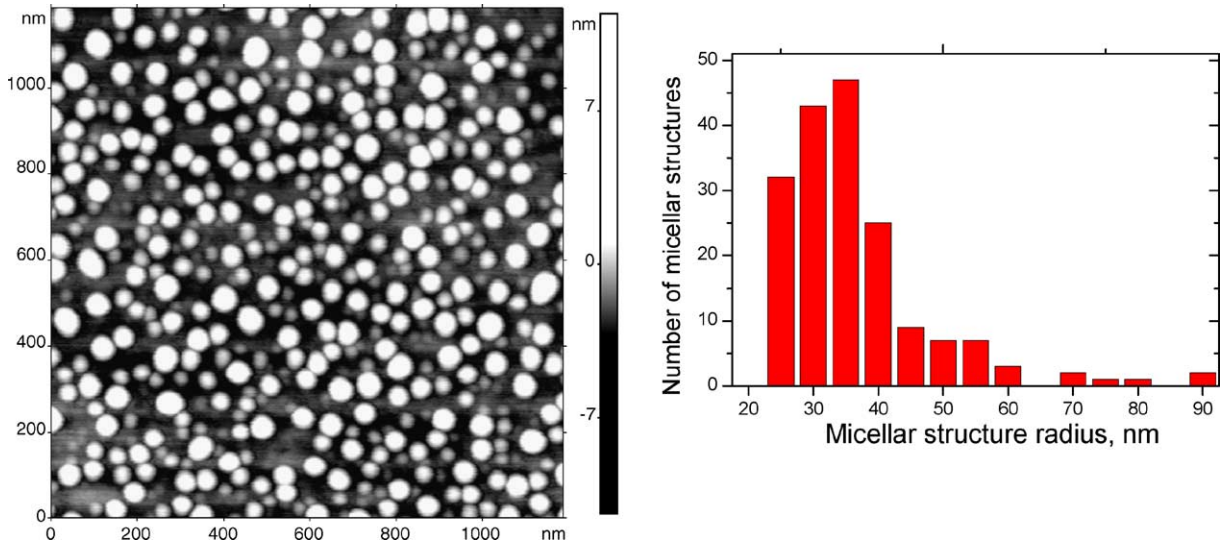

Fig. 5. AFM image (left) and size histogram (right) for the sample 2 from Table 1.

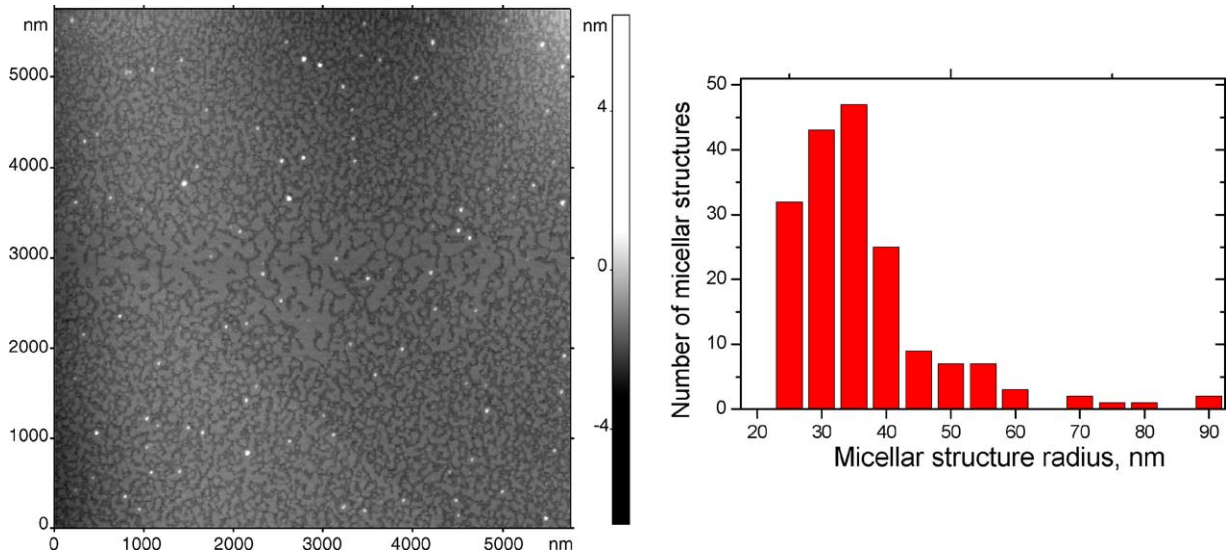

Fig. 6. AFM image (left) and size histogram (right) for the sample 3 from Table 1.

(a few micelles in each cluster). By AFM data (Fig. 5), a mean diameter of the micelles is 34 nm. (One should consider that for small micelles, no absolute value of micelle size could be derived from the AFM data, as the probe tip size was not evaluated). The density of the majority of the micelles (Fig. 2b) is rather low. These structures result in a high activity, but comparatively low selectivity. The sample 3 (Fig. 2c) shows two types of structures: small spherical micelles (13–20 nm in diameter) which are embedded in huge micellar aggregates measuring up to 800 nm and other very low density aggregates of approx. 600 nm in diameter. Apparently, presence of small micelles embedded in loose aggregates ensures high activity of this sample, while comparatively high density of the micelles leads to high selectivity. AFM data for the sample 3 (Fig. 6) confirm formation of large micellar aggregates along with small ones with a mean diameter of 70 nm, while small "embedded" micelles are not seen. Thus, the negative influence of large micellar aggregates (comparing to the sample 2) on activity is counterbalanced by better transport of DHL to the Pd nanoparticles in small micelles. Increased selectivity of the sample 3 can be caused by denser micelles (than for sample 2) and positive influence of *i*-PrOH that may block multiple adsorption sites responsible for the selectivity deterioration [35,48].

In the sample 4 (Fig. 2d), one can see smaller and denser micelles and denser aggregates than in the sample 3. The AFM image (Fig. 7) shows very small micelles (a mean diameter of 28 nm) which are prone to aggregation. Higher density ensures the increase of selectivity and decrease in

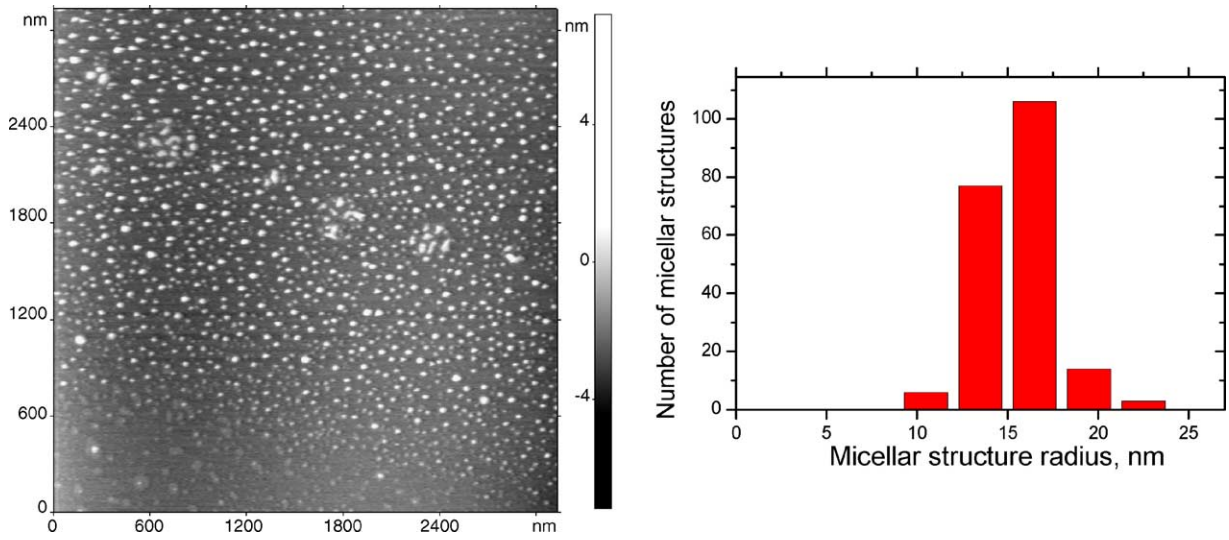

Fig. 7. AFM image (left) and size histogram (right) for the sample 4 from Table 1.

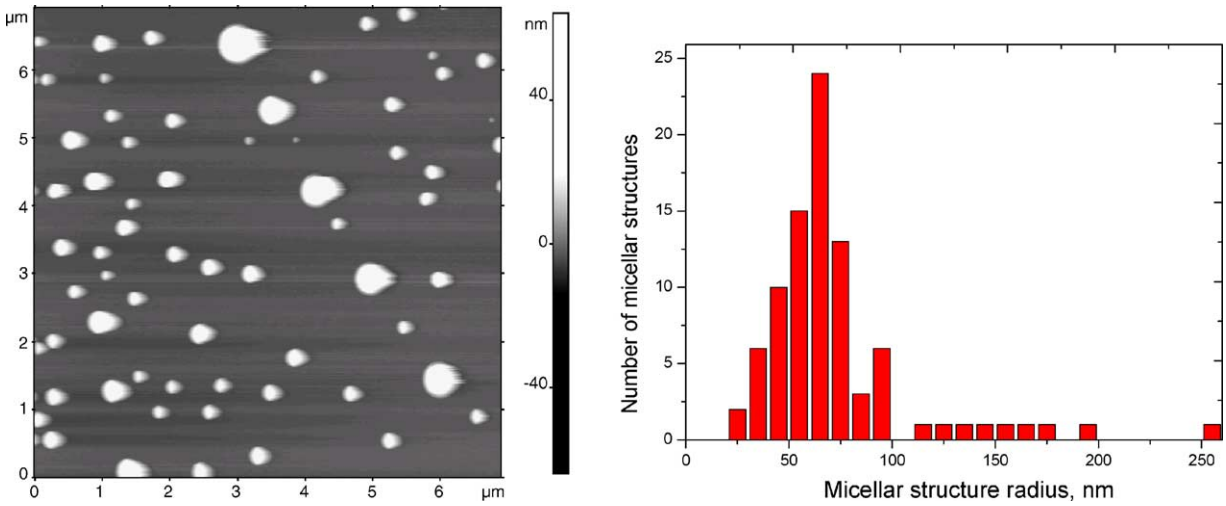

Fig. 8. AFM image (left) and size histogram (right) for the sample 12 from Table 1.

activity. Comparison of the TEM images of the samples 3 and 6 (Figs. 2c and 3a) shows that additional KOH (sample 6) leads to more complex system displaying several levels of micelle organization, when micellar structures are embedded in each other, which decreases both activity and selectivity. On the other hand, micellar aggregates seen in Fig. 3a can be secondary structures formed on the electron grid. The AFM image of the sample 6 (Fig. 9) shows micelles with a mean diameter of 86 nm.

For comparison, average diameters of micellar structures for the samples 3 and 6 in reaction solutions were obtained from turbidity spectra [39] and measure 216 and 196 nm, respectively. These data confirm the presence of large aggregates, although they should not be considered as a correct quantitative characteristic of the micellar solutions. When a solution contains a few large aggregates, the mean diameter is strongly influenced while catalytic properties are determined by the size of the majority of the micelles.

Despite the dominating influence of the micelle characteristics on catalytic properties demonstrated above, comparison of the samples 4 and 6 shows that additional factors should be taken into consideration. Although the sample 6 has much larger micelles and micellar aggregates than the sample 4 (Figs. 2d and 3a), the former displays higher activity than the latter that may be explained by the positive influence of KOH: electron donation to Pd [35].

In addition, water can also adsorb on the Pd surface [49] and cause changes in selectivity and activity but the experimental results, e.g. the data for the samples 2–4, do not confirm such a simple water influence. Possible *i*-PrOH decomposition on the catalyst surface [50] or its dehydrogenation to acetone [51] can be excluded as GC examination of the reaction mixtures did not show any of the possible products.

When nearly pure *i*-PrOH (0.1 ml water are introduced with a block copolymer sample) is used (sample 12, Fig. 3b),

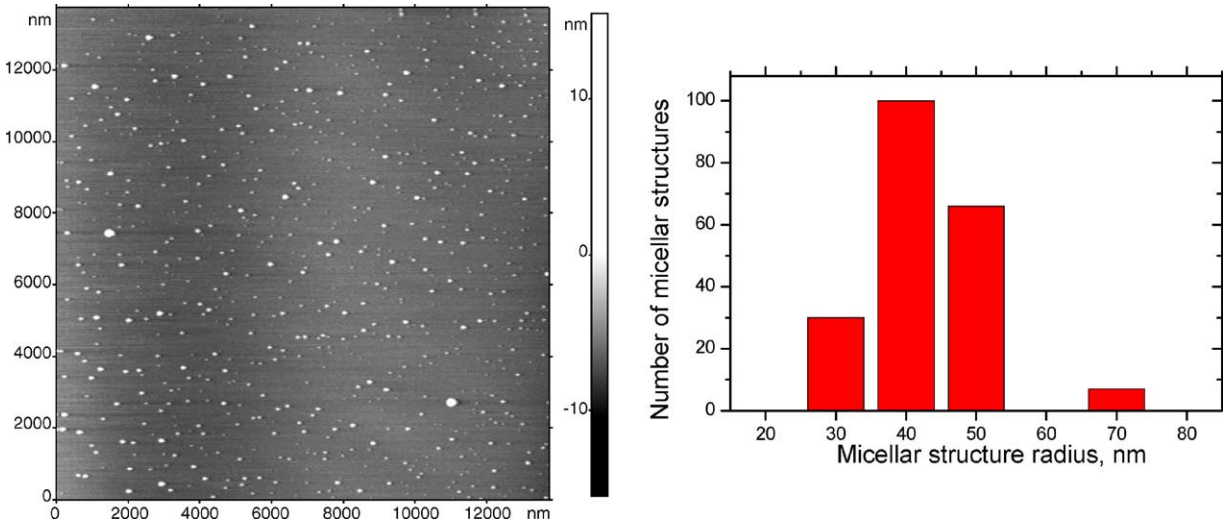

Fig. 9. AFM image (left) and size histogram (right) for the sample 6 from Table 1.

the major part of the sample contains very dense micelles inclining to further aggregation which results in the dramatic activity deterioration. The AFM image of the sample 12 (Fig. 8) shows micelle aggregates with a mean diameter of 144 nm.

Thus, changes of micellar characteristics (caused by change of solvent composition and pH) seem to be major factors, which are responsible for variation of catalytic properties in these systems due to presence or absence of internal diffusion limitations, although the influence of KOH and *i*-PrOH as catalyst modifiers are of importance as well. It is noteworthy that micellar characteristics influence significantly the catalytic activity, while selectivity values stay comparatively high (in the range of 94.2–100%) due to permanent modification of Pd nanoparticles with pyridine units in the micelle core.

Selective DHL hydrogenation was also studied under external diffusion limitations (480 oscillations/min) for the sample 3 from Table 1. At 480 oscillations/min the selectivity was 98.4 ± 0.3% at 100% DHL conversion that is higher than the one at 960 oscillations/min. In general, diffusion limitations are known to decrease the selectivity in acetylene hydrogenation [52]. At the same time, for DHL hydrogenation with another colloidal catalyst described in [28], we showed earlier an increase of selectivity in the diffusion limitation regime. The same results were obtained in hydrogenation of other long chain acetylene alcohols with the catalyst Pd/Al_2O_3 [35]. The reason for such an effect in a system with diffusion limitations may lie in a lower quantity of bulk (absorbed) hydrogen per unit time comparing to effective stirring. Bulk hydrogen is known to be responsible for non-selective hydrogenation [53]. It should be noted that the increased selectivity at the decreased reaction rate, shown for the reaction conducted at external diffusion limitations, was also observed for some samples at 960 oscillations/min (e.g. the samples 4 and 13) indicating once again mass transport effects.

Thus, micelle characteristics depending on the pH and the '*i*-PrOH:water' ratio play an important role in the catalytic properties as they may control the substrate and product transport toward and from active centers and their modification. The influence of the solvent resembles the results reported on the behavior of resin-supported palladium catalysts in alkene hydrogenation [18]. There, the substrate interaction with polymer chains, leading to a high barrier for diffusion throughout the polymer, was suppressed by using a reaction solvent (methanol) fully solvating the polymer chains. In a similar way, *i*-PrOH can solvate the P2VP micelle core causing its swelling and the better mass transport of DHL throughout the micelles, although the studied system seems to be much more complex than the one in [18] and the *i*-PrOH influence (along with KOH) is more complicated as well. As discussed above, an additional role of *i*-PrOH and KOH in the reaction mixture can be electronic and geometric modification of the catalyst surface, however our results display only a few examples of this influence once again due to complexity of this system.

3.3. Kinetic study

Kinetics of selective DHL hydrogenation was studied for the reaction carried out at a pH of 14.3 and 70 vol.% *i*-PrOH in a mixed solvent (the sample 8, Table 1), as these conditions provide comparatively high selectivity (98.0 ± 0.2% at 100% DHL conversion) at high specific rate. The system chosen for studying the kinetics must be free of diffusion limitations. Taking into consideration that the specific rate for this system is equal to that of the sample 2 from Table 1 (containing small low-density micelles with a mean diameter of 34 nm and no large aggregates), i.e. the specific rate for these two systems is independent of the micellar characteristics, it may be considered as intrinsic reaction rate. The latter means that hydrogenation with the sample 8 is free of mass transport effects so this sample is suitable for kinetic study. The apparent activation energy of the reaction conducted at substrate-to-catalyst ratio = 23,302 was determined from the reaction rate values found at 50% conversion in the temperature range of 50–70 °C. Its value deduced from the slope of the Arrhenius equation was found to be 31.2 ± 0.2 kJ/mol. Other kinetic experiments were carried out at 70 °C varying SCR values (C_0 and C_c were varied in the ranges of 0.21–0.58 mol/l and 1.6×10^{-5} to $1.8\cdot10^{-5}$ mol of Pd/l, respectively).

Fig. 10a shows the dependencies of DHL conversion versus the reaction time τ at different C_0 and C_c values. Standard deviations were in the range of ±(0.3–0.8%). The kinetic curves obtained at different SCRs were brought together, for this purpose the abscissa was normalized to relative time (θ) which values were calculated from the current reaction time:

$$\theta = \frac{\tau}{\mathrm{SCR}}. \tag{4}$$

The DHL consumption specific rate (r) in a batch reactor can be presented as

$$rC_c = -\frac{\mathrm{d}C_{\mathrm{DHL}}}{\mathrm{d}\tau}, \tag{5}$$

or, dividing by initial DHL concentration and indicating $X_{\mathrm{DHL}} = (C_{\mathrm{DHL}}/C_0)$

$$r = -\frac{\mathrm{d}X_{\mathrm{DHL}}}{\mathrm{d}\theta}. \tag{6}$$

Fig. 10b shows the kinetic data as the dependence of DHL conversion (i.e. $(1 - X_{\mathrm{DHL}}) \times 100\%$) on relative time θ. One can see the existence of the initial phase characterized by low reaction rate (up to approx. 20% DHL conversion). Remarkably, during this phase the selectivity remained 100% with the following drop to 98.0 ± 0.5%; after that the selectivity remained constant. This fact is in agreement with conclusions that during the initial phase of the alkyne hydrogenation over Pd, both reactive and less

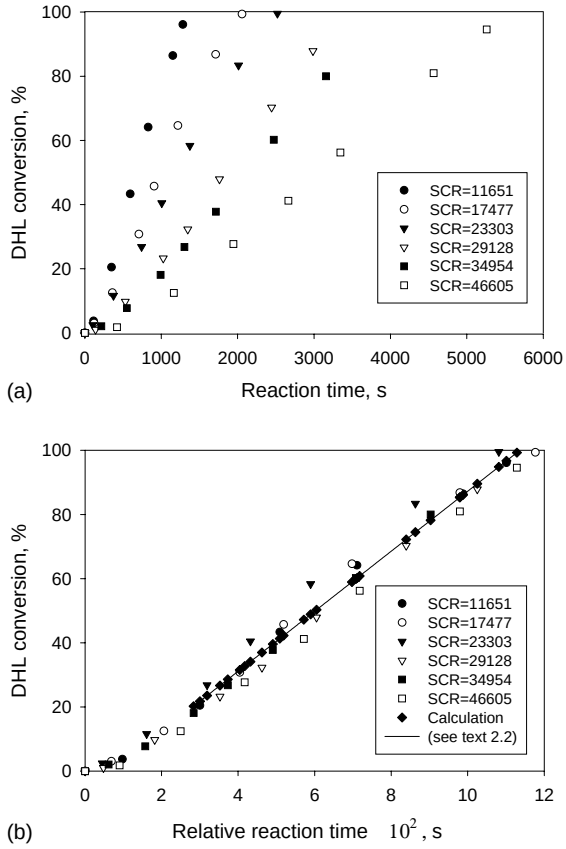

Fig. 10. Dependencies of DHL conversion vs. reaction time (a) and vs. relative time (b) at different SCR values. Solid line indicates the calculated linear dependence; the initial phase (up to 20% DHL conversion) was not taken into consideration. Reaction conditions: 960 oscillations/min, 70 °C, pH 14.3, 70 vol.% *i*-PrOH.

reactive surface species are formed and that less reactive ones are responsible for high selectivity [22,54]. Thus, we can assume that during the initial phase, the reaction proceeds via less reactive species yielding 100% selectivity, while highly reactive species responsible for the selectivity drop are being formed. After the initial phase, one can see a linear dependence indicating zero order with respect to DHL, which is often related to the strong adsorption of the substrate on the catalyst surface [55]. The DHL consumption specific rate was confirmed to be constant and equal to 9.4 ± 0.3 mol DHL/(mol Pd s) for all the studied SCRs.

3.4. TOF calculation

To compare the activity of the catalysts described in this paper with other catalysts reported (for example, [56]), we calculated a TOF value for the reaction carried out as the run 5 in Table 1. Traditionally, the TOF should be calculated as moles of DHL consumed per second per mol of available active sites [57], however, the estimation of the latter presents a serious problem [58]. Even if one determines the amount of binding sites for a certain gas, the number of these sites may be different from those that actually catalyze the reaction [59]. Thus, in our first approximation, we assumed that the number of moles of surface atoms is equal to the number of moles of active sites, as is done in [60].

To determine the number of surface Pd atoms, we have used an approach described in [57] and formulas proposed by Benfield [61]. For spherical Pd nanoparticles similar to those shown in the inset of Fig. 2a, Li et al. [57] assumed that the nanoparticles are cuboctahedral in shape with a cubic close packed structure and concentric shells of atoms. As suggested in [62], such a Pd nanoparticle with a mean diameter of 25 Å (as is in our case) corresponds to a five-shell structure around one single central atom. According to formulas presented in [61], for the number of shells $m = (5+1)$ (the central atom is assigned as $m = 1$) the total number of atoms in one nanoparticle is 561, and the number of surface atoms in this nanoparticle is 252. As 5.657×10^{-7} mol of Pd atoms are used in the reaction, the reaction mixture contains 1.008×10^{-9} mol of Pd nanoparticle or 2.541×10^{-7} mol of surface Pd atoms. For the run 5 (Table 1), where 1.314×10^{-2} DHL moles were fully converted for 2117 s, the average TOF is 24.4 s^{-1}. As the active site could consist of more than one surface atom, the TOF value might be even higher. Nevertheless, it is one of the highest reported for acetylene hydrogenation. For example, TOF of Pd/α-Al_2O_3 (0.01% Pd) in acetylene hydrogenation to ethylene is 4.8 s^{-1} [56], that is five-fold lower than the reported value.

In the second approximation for TOF calculation, we used an assumption made by Niessen et al. [63] who have studied hydrogenation of 3-methyl-1-pentyne-3-ol (which is similar to DHL) with Pd nanoparticle formed in PS-*b*-P4VP micelles, and visualized the active site as the one consisting of seven Pd atoms (one central atom and six around the central one). If we presume that, in our case, an active site consists of seven Pd atoms as well, then the TOF is equal to 171 s^{-1} that is one of the highest known in catalysis, especially taking into account the substrate complexity.

4. Conclusions

Pd nanoparticles with a mean diameter of 2.5 nm formed in the PEO-*b*-P2VP micelles show catalytic activity and selectivity in DHL hydrogenation. The catalytic properties of this system were found to depend on the solvent composition ('*i*-PrOH:water' ratio) and pH of the medium, as these parameters influence the micelle characteristics of the PEO-*b*-P2VP–Pd system. The micellar parameters control diffusion and adsorption of DHL and hydrogen, and diffusion and desorption of LN within the micelles, thus, alter the reaction rate and selectivity. The denser the micelles, the higher the pyridine unit local concentration (which increases selectivity) and the slower the DHL diffusion within the micelles (which decreases the reaction rate). The highest selectivity (99.4%) was obtained at pH of 9.4 and 95 vol.% of *i*-PrOH. The highest observed TOF value calculated as moles of DHL consumed per second per mole of surface Pd

atom was found to be 24.4 s^{-1} at pH of 13.0 and 70 vol.% of *i*-PrOH. KOH and isopropanol were shown to affect both the micelle characteristics and act as electronic and geometric modifiers of the catalyst surface.

According to [64], use of noble metals in the fragrance and flavor industry is only justified when TOF is higher than 1000 or 10,000 h^{-1} (0.3 or 2.8 s^{-1}, respectively) depending on the cost of the target product. Here we reported much higher TOF which allows proposing this catalyst for linalool preparation especially that the micellar catalyst shows an excellent colloidal stability (does not change micellar characteristics for months). For the better technological performance, PEO-*b*-P2VP–Pd can be deposited from the micellar solutions on various supports, e.g. γ-Al_2O_3, to give heterogeneous catalysts. This would allow the recycling of the catalyst, although the excellent catalytic activity might be decreased. The properties and behavior of the heterogeneous PEO-*b*-P2VP–Pd catalysts is a subject of our current study and will be reported in a future publication. We believe this catalyst has a great potential for various catalytic reactions where use of water–alcohol mixtures or water as a solvent is appropriate.

Acknowledgements

We sincerely thank NATO Science for Peace Programme (grant SfP-974173) and Russian Foundation for Basic Research (grant RFBR- 01-03-32937) for financial support of this research. We wish also thank Prof. J.W. Zwanziger for help with resources and instruments.

References

[1] R. Brayner, G. Viau, F. Bozon-Verduraz, J. Mol. Catal. A 182–183 (2002) 227.
[2] C. Liu, Y. Xu, S. Liao, D. Yu, J. Mol. Catal. A 157 (2000) 253.
[3] A. Drelinkiewicz, M. Hasik, M. Kloc, J. Catal. 186 (1999) 123.
[4] B. Veisz, Z. Kiraly, L. Toth, B. Pecz, Chem. Mater. 14 (2002) 2882.
[5] M. Kralik, A. Biffis, J. Mol. Catal. A: Chem. 177 (2001) 113.
[6] K. Okitsu, A. Yue, S. Tanabe, H. Matsumoto, Chem. Mater. 12 (2000) 3006.
[7] A. Horvath, A. Beck, A. Sarkany, L. Guczi, Solid State Ionics 148 (2002) 219.
[8] S.N. Sidorov, I.V. Volkov, V.A. Davankov, M.P. Tsyurupa, P.M. Valetsky, L.M. Bronstein, R. Karlinsey, J.W. Zwanziger, V.G. Matveeva, E.M. Sulman, N.V. Lakina, E.A. Wilder, R.J. Spontak, J. Am. Chem. Soc. 123 (2001) 10502.
[9] J.F. Ciebien, R.T. Clay, B.H. Sohn, R. Cohen, New J. Chem. 22 (1998) 685.
[10] H. Xiong, Z. Zhou, Z. Wang, Z. Xi, J. Shen, Supramol. Sci. 5 (1998) 623.
[11] L.M. Bronstein, O.A. Platonova, A.N. Yakunin, I.M. Yanovskaya, P.M. Valetsky, A.T. Dembo, E.S. Obolonkova, E.E. Makhaeva, A.V. Mironov, A.R. Khokhlov, Colloids Surf A 147 (1999) 221.
[12] Z. Lu, G. Liu, H. Phillips, J.M. Hill, J. Chang, R.A. Kydd, Nano Lett. 1 (2001) 683.
[13] M. Zhao, R.M. Crooks, Adv. Mater. 11 (1999) 217.
[14] M. Antonietti, E. Wenz, L. Bronstein, M. Seregina, Adv. Mater. 7 (1995) 1000.
[15] J.P. Spatz, A. Roescher, M. Möller, Adv. Mater. 8 (1996) 337.
[16] M. Moffitt, L. McMahon, V. Pessel, A. Eisenberg, Chem. Mater. 7 (1995) 1185.
[17] M. Kralik, A. Biffis, J. Mol. Catal. A 177 (2001) 113.
[18] M. Zecca, R. Fisera, G. Palma, S. Lora, M. Hronec, M. Kralik, Chem. Eur. J. 6 (2000) 1980.
[19] M.V. Seregina, L.M. Bronstein, O.A. Platonova, D.M. Chernyshov, P.M. Valetsky, J. Hartmann, E. Wenz, M. Antonietti, Chem. Mater. 9 (1997) 923.
[20] H. Molero, B.F. Barlett, W.T. Tysoe, J. Catal. 181 (1999) 49.
[21] E.S. Mirzoeva, L.M. Bronstein, P.M. Valetsky, E.M. Sulman, React. Polym. 24 (1995) 243.
[22] A. Molnar, A. Sarkany, M. Varga, J. Mol. Catal. A 173 (2001) 185.
[23] V.V. Rusak, M.I. Zaretskii, A.S. Mozzhukhin, I.V. Usyshkina, L.A. Pushkina, Russ. J. Appl. Chem. 67 (1994) 1066.
[24] S. Pattnaik, V.R. Subramanyam, M. Bapaji, C.R. Kole, Microbios 89 (1997) 39.
[25] H. Lindlar, Helv. Chim. Acta 35 (1952) 446.
[26] L. Uhlar, M. Polievka, M. Kavala, CS 253436, Chem. Abstracts 110:233625, 1988.
[27] E. Sulman, Y. Bodrova, V. Matveeva, N. Semagina, L. Cerveny, V. Kurtc, L. Bronstein, O. Platonova, P. Valetsky, Appl. Catal. A 176 (1999) 75.
[28] L.M. Bronstein, D.M. Chernyshov, I.O. Volkov, M.G. Ezernitskaya, P.M. Valetsky, V.G. Matveeva, E.M. Sulman, J. Catal. 196 (2000) 302.
[29] Z.M. Michalska, B. Ostaszewski, J. Zientarska, J.W. Sobczak, J. Mol. Catal. A 129 (1998) 207.
[30] J.P. Boitiaux, J. Cosyns, S. Vasudevan, Appl. Catal. 15 (1985) 317.
[31] R.E. Fredricks, J. Appl. Polym. Sci. 57 (1995) 509.
[32] H.-C.B. Chen, L.M. Czupski, J. Adh. Seal. Council 1 (1996) 205.
[33] A.M. Pak, O.I. Kartonozhkina, Y.L. Sheluduakov, in: Proceedings of the Ninth International Symposium on Relations between Homogeneous and Heterogeneous Catalysis, Southampton, UK, 20–24 July 1998, p. 123.
[34] T.J. Martin, K. Prochazka, P. Munk, S.E. Webber, Macromolecules 29 (1996) 6071.
[35] E.M. Sulman, Russ. Chem. Rev. 63 (1994) 923.
[36] L.M. Bronstein, S.N. Sidorov, P.M. Valetsky, J. Hartmann, H. Coelfen, M. Antonietti, Langmuir 15 (1999) 6256.
[37] A. Stemmer, A. Engel, Ultramicroscopy 34 (1990) 129.
[38] W. Heller, W.J. Pangonis, J. Chem. Phys. 26 (1957) 498.
[39] W. Heller, H.L. Bhatnagar, M. Nakagaki, J. Chem. Phys. 36 (1962) 1163.
[40] Z. Dobrovolna, P. Kacer, L. Cerveny, J. Mol. Catal. A: Chem. 130 (1998) 279.
[41] A. Biffis, B. Corain, Z. Cvengrosova, M. Hronec, K. Jerabek, M. Kralik, Appl. Catal. A 142 (1996) 327.
[42] S. Jayasree, A. Seayad, B.R. Sarkar, R.V. Chaudhari, J. Mol. Catal. A 181 (2002) 221.
[43] M.M. Telkar, C.V. Rode, V.H. Rane, R. Jaganathan, R.V. Chaudhari, Appl. Catal. A 216 (2001) 13.
[44] L. Fabre, P. Gallezot, A. Perrard, Catal. Commun. 2 (2001) 249.
[45] D. Duca, F. Arena, A. Parmaliana, G. Deganello, Appl. Catal. A 172 (1998) 207.
[46] E.W. Shin, C.H. Choi, K.I. Chang, Y.H. Na, S.H. Moon, Catal. Today 44 (1998) 137.
[47] L. Fabre, G. Fleche, P. Fuertes, P. Gallezot, A. Perrard, Catal. Lett. 68 (2000) 41.
[48] S. Leviness, V. Nair, A.H. Weiss, Z. Schay, L. Guczi, J. Mol. Catal. 25 (1984) 131.
[49] D.L. Mowery, M.S. Graboski, S. Michael, T.R. Ohno, R.L. McCormic, Appl. Catal. B 21 (1999) 157.
[50] G.A.M. Hussein, N. Sheppard, M.I. Zaki, R.B. Fahim, J. Chem. Soc., Faraday Trans. 185 (1989) 1723.

[51] J.L. Davis, M.A. Barteau, Surf. Sci. 187 (1987) 387.
[52] S. Asplund, C. Fornell, A. Holmgren, S. Irandoust, Catal. Today 24 (1995) 181.
[53] Q. Zhang, J. Li, X. Liu, Q. Zhu, Appl. Catal. A 197 (2000) 221.
[54] P. Maetz, R. Touroude, Appl. Catal. A 149 (1997) 189.
[55] P.A. Rautanen, J.R. Aittamaa, A.O.I. Krause, Ind. Eng. Chem. Res. 39 (2000) 4032.
[56] R.K. Edvinsson, A.M. Holmgren, S. Irandoust, Ind. Eng. Chem. Res. 34 (1995) 94.
[57] Y. Li, E. Boone, M.A. El-Sayed, Langmuir 18 (2002) 4921.
[58] G.C. Bond, A.F. Rawle, J. Mol. Catal. 109 (1996) 261.
[59] J.W. Yoo, D.J. Hathcock, M.A. El-Sayed, J. Catal. 214 (2003) 1.
[60] J. Le Bars, U. Specht, J.S. Bradley, D.G. Blackmond, Langmuir 15 (1999) 7621.
[61] R.E. Benfield, J. Chem. Soc., Faraday Trans. 88 (1992) 1107.
[62] T. Teranishi, M. Miyake, Chem. Mater. 10 (1998) 594.
[63] H.G. Niessen, A. Eichhorn, K. Woelk, J. Bargon, J. Mol. Catal. A 182–183 (2002) 463.
[64] C. Chapuis, D. Jacoby, Appl. Catal. A 221 (2001) 93.